M. JENKO, D. MANDRINO, M. MILUN

ISSN 0543-5846
METABK 41 (3) 191 (2002)
UDC - UDK 669:543.42AUGER=20

HIGH RESOLUTION AUGER SPECTROSCOPY IN METALLURGY: AN ADVANCED TECHNIQUE FOR SURFACE ANALYSIS

Received - Primljeno: 2002-03-10
Accepted - Prihvaćeno: 2002-05-15
Review Paper - Pregledni rad

A brief review of the high spatial resolution Auger electron spectroscopy (HRAES) and its usage in metallurgy is presented. A combination of HRAES and X-ray photoelectron spectroscopy makes a powerful combination to resolve a large number of problems encountered in metallurgy. Several selected examples of such problems studied in the authors' laboratory are presented: influence of surface active impurities on the surface properties and structure, chemical composition of nano-scaled inclusions, homogeneity of oxide layers formed by decarburization, chemical composition of inter- and intra-grain surfaces obtained by fracture in vacuum and interfacial study of 19Cr-13Ni austenitic stainless steel after treatment at elevated temperatures.

Key words: *Auger spectroscopy, surface analysis, high resolution*

Auger-spektroskopija visoke resolucije u metalurgiji: moderna tehnika površinske analize. Predočen je kratki pregled Auger-ove elektronske spektroskopije (HREAS) visoke spacijalne resolucije i njene primjene u metalurgiji. Kombinacija HREAS i röntgenske fotoelektronske spektroskopije učinkovita je pri rješavanju velikog broja problema koji se susreću u metalurgiji. Predočeno je nekoliko odabranih primjera takvih problema studiranih u laboratoriju autora: utjecaj površinski aktivnih nečistoća na svojstva i strukturu površine, kemijski sastav "nano-uključaka", homogenost oksidnih slojeva nastalih odugljičenjem, kemijski sastav površina u zrnu i među zrnima nastalih lomljenjem u vakuumu te međufazna studija 19Cr-13Ni nehrđajućeg austenitnog čelika nakon obrade kod povišenih temperatura.

Ključne riječi: *Auger-ova spektroskopija, površinske analize, visoka resolucija*

INTRODUCTION

A considerable contribution to the advancement of metallurgy has been made by surface analysis in particular by using Auger electron spectroscopy (AES) and X-ray-photoelectron spectroscopy (XPS) [1]. In characterizing of material, perhaps the most important special area of interest is surface.

These techniques are frequently used to study corrosion, oxidation, carbonization, nitridation, soldering, sintering and at powder metallurgy, wear and development of hard metals and heavy metals as well as a wide range of general interfacial problems in single phase, multiphase and composite materials.

High resolution Auger electron spectroscopy (HRAES) has three well-defined advantages over Electron probe microanalysys (EPMA) at traditional microanalysis: a) submicron spatial resolution, b) good detection for light elements except hydrogen and helium and c) in combination with ion sputtering it enables one to perform depth profile analysis of the sample. These extremely important advantages account for considerable industrial work with high resolution Auger electron spectroscopy.

A recent advance in Auger electron spectroscopy has been the addition of field emission gun (FEG) electron source to standard commercial instruments for routine use. Traditionally, emphasis has been placed on the spectroscopic information that is obtained by the technique, rather than exploring its microscopic analytical and imaging potentials. If a FEG source is used in conjunction with an efficient electron spectrometer, a beam diameter of a few tens of nanometers and a typical beam current of 1-10 nA can be used for routine analysis. This beam current will excite a secondary electron yield that is sufficient to allow high quality scanning electron microscope SEM images

M. Jenko, D. Mandrino, M. Milun, Institute of Metals and Technology, Ljubljana, Slovenia

to be recorded. The scanning capability of the beam combined with its nano-spot beam offer a possibility to perform scanning Auger microscopy (SAM). This is accomplished by monitoring the intensity change of a particular Auger electron intensity across the surface. If, for example, the distribution of carbon is of interest one would monitor the intensity of the C KLL Auger electron of 273 eV kinetic energy as a function of the beam position on the surface [2]. The Auger map thus obtained reveals the true distribution of carbon on a nanoscale. In our case this would be about 10 nm lateral resolution.

In both, AES and XPS the information originate from the sample depth determined by the Auger- or photo-electron mean free path and this is a function of the electron kinetic energy. For the typical kinetic energy range of 0 - 2000 eV the electron mean free path may range [1] from several tenths to several tens of nm. This makes both spectroscopes very surface sensitive.

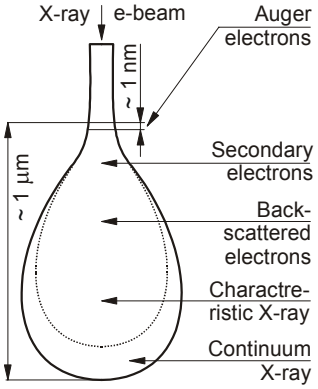

Figure 1. **Schematic diagram showing interaction of electron beam with bulk sample surface, depth of origin of various signals is indicated**

Slika 1. **Shematski dijagram koji ukazuje na interakciju elektronskog snopa s volumenom blizu površine uzorka. Naznačena je dubina na kojoj nastaju razni signali**

Figure 1. shows a schematic illustration comparing the origin of the X-ray and Auger analytical signals. Note that the penetration depth of an electron beam of several keV energy, as is typical for AES, significantly exceeds the electron mean free path values. However, a number of electrons from the irradiated space will leave the sample and enter the analyzer. During the travel they loose energy in a number of inelastic events. They form a large, so called secondary electron background in AES and XPS spectra [1, 3, 4].

The Auger electron can be excited by using an electron beam or a beam of photons. For the purpose of high spatial resolution, i. e., very small spot size for analysis it is needed to use an electron beam source (of high intensity) because of the problems associated with focusing of a photon beam.

In metallurgy, material characterization on a sub-micron scale is often an essential information to understand material behavior. It is very much so in situations where inclusions, grain boundaries, and other inhomogeneities essentially influence properties of the substance under study. The high surface sensitivity of HRAES may at first glance be taken as a disadvantage when one seeks to get an insight in the bulk properties of the metallic sample. However, this is not so because a technique of *in situ* (in ultra high vacuum- UHV) fracture of a specimen is nowadays routinely available. By fracturing the sample at UHV condition fresh transcrystal - and intercrystal facets, grain boundaries and phases are exposed to examination. In such a way, truly bulk material as well as phenomena on grain boundaries and phases may be studied.

In this paper we present several typical examples where HRAES and XPS are used to resolve problems related to metallurgy.

EXPERIMENTAL PROCEDURE

The spectrometer is a Vacuum Generators Microlab 310-F instrument composed of two ultrahigh vacuum chambers, one for the sample preparation and one for the spectroscopic studies. The Auger electron spectrometer has a thermally assisted Schottky field emission source that provides a stable electron beam in the accelerating voltage range of 0.5 to 25 keV.

The electron analyser is of a double focusing spherical sector type with an electrostatic input lens and can provide energy resolution between 0.02% and 2%.The spec-

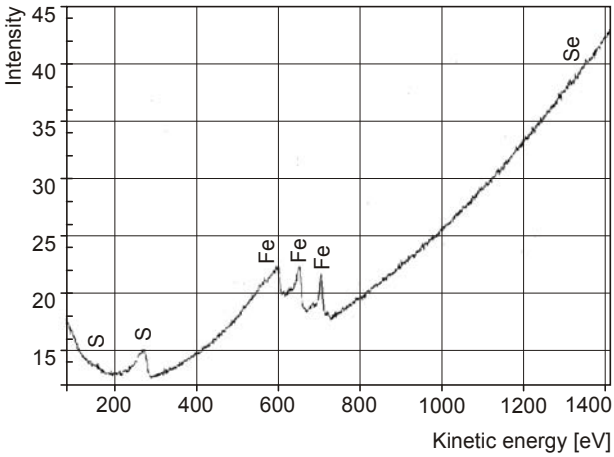

Figure 2. **Auger spectrum of an FeSi alloy at equilibrium Se-S segregation at T ≥ 800 °C**

Slika 2. **Auger-ov spektar FeSi legure pri ravnotežnoj Se-S segregaciji na T ≥ 800 °C**

trometer has five sequential channeltrons (electron detectors), each of which detects 2.5% of the pass energy. Spectra are mostly acquired with a constant retard ratio (CRR) of 4 which provides an energy resolution that is 0.5% of the pass energy. At a fixed pass energy channeltrons can be assigned separately to provide peak or background signals for simultaneous elemental mapping. The instrument is additionally equipped with an X-ray source (Mg, Al dual anode) which in combination with the electron energy analyser forms an XPS photoelectron spectrometer for surface chemical analysis.

SOME SELECTED EXAMPLES

Selenium segregation

Segregation of low-concentration or impurity elements that exhibit surface activity may significantly influence surface properties of the material under study. An example is FeSi with added small concentration (app. 0.05 mass.%) of Se. Selenium, being a surface active element [5-8] induces surface recrystallization of the FeSi sheet [9]. Figure 2. shows an Auger spectrum of the polycrystalline FeSiSe sample at a maximum Se level after the segregation process was completed at 800 °C. Beside selenium sulfur segregated as well. After several runs from 500 to 850 °C the saturation value for both S and Se was reached. AES depth profile analysis shown in Figure 3. indicated that selenium saturated surface enrichment was about 10 at. % and sulfur about 20 at. % and that there is no selenium in the layers near the surface. It was also clear that the observed phenomenon was not a competition between Se and S for the free sites on the surface because the ratio

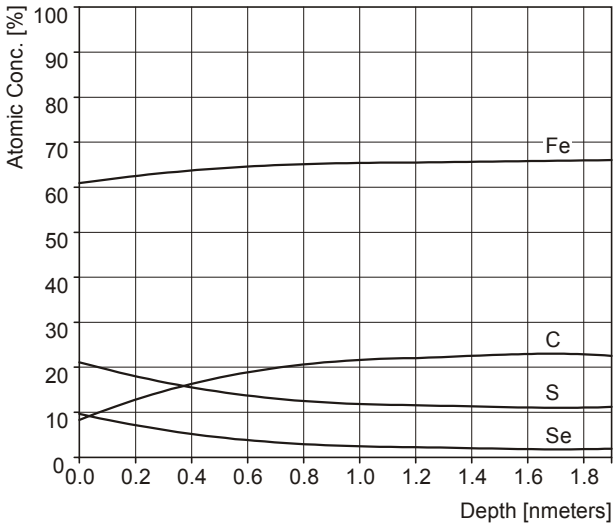

Figure 3. **The AES depth profile of near-surface composition of an FeSi alloy (with Se-S segregation) which was annealed at T ≥ 800 °C. The depth profile was obtained at room temperature**

Slika 3. **AES dubinski profil sastava blizu površine FeSi legure (pri segregiranom Se-S) napuštene pri T ≥ 800 °C. Dubinski je profil dobiven pri sobnoj temperaturi**

Se-S was equal in all runs. A possible explanation could be either parallel segregation of Se and S or the formation of a S-Se surface compound. The dilemma was resolved by analysis of the XPS data. The Se(3s), S (2s) and Fe ($2p_{1/2}$) and Fe ($2p_{3/2}$) core level photoelectron intensities from saturated sample are shown in Figure 4. The measured binding energies are 230.6 eV (characteristic for pure Se), 227.9 eV (characteristic for pure S), 707.0 eV and 720.1 eV (characteristic for pure Fe), respectively. Evi-

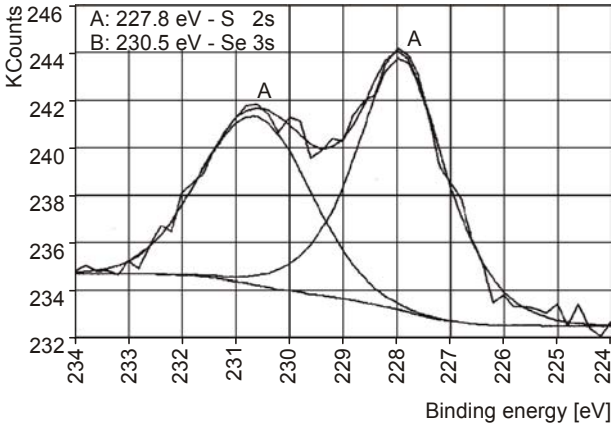

Figure 4. **a) XP spectra (MgKα radiation, 1253.6 eV) of an FeSi alloy. The Se 3s and S 2s photoelectron lines were measured at the equilibrium of surface segregation (T ≥ 800 °C). The measured binding energies for both lines (Se at 230.5 eV and S at 227.8 eV) are characteristic of those of the pure elements**
b) The Fe $2p_{1/2}$ and Fe $2p_{3/2}$ XPS lines for the same sample as in a). These line energies are characteristic of pure iron

Slika 4. **a) XP spektar (MgKα , 1253.6 eV) FeSi legure. Se 3s i S 2s fotoelektronske linije mjerene su u ravnoteži površinske segregacije (T ≥ 800 °C). Mjerene energije vezanja za obje linije (Se pri 230.5 eV i S pri 227.8 eV) su karakteristične za čiste elemente**
b) Fe $2p_{1/2}$ i Fe $2p_{3/2}$ XPS linije za isti uzorak kao u a). Energije tih linija su karakteristične za čisto željezo

dently neither Se-S nor Fe-Se-S surface compounds are formed during the co-segregation process.

The grain growth and micromorphology of the sample surface was monitored in situ by SEM. After several runs at 850 °C the microstructure changed drastically and on some grains the faceting occurred. It is known that faceting occurs if the new planes are energetically favored despite of their increased total area, according to the tendency of a crystal to decrease its surface energy. Even on single

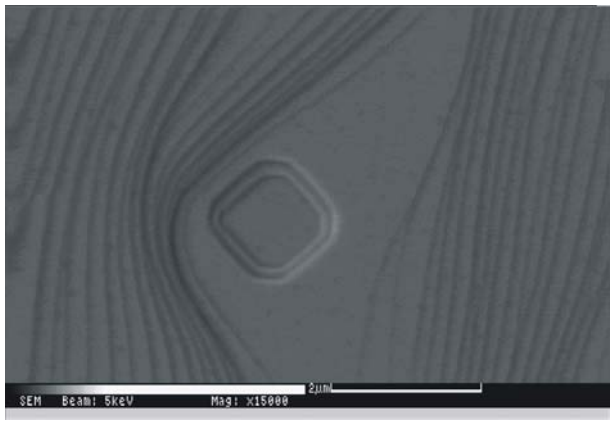

Figure 5. **The SEM image of the first stage of surface reconstruction of (110) to (100) grains planes which occurred during Se-S co-segregation.**

Slika 5. **SEM slika prvog stupnja površinske rekonstrukcije (110) u (100) ravninu zrna koja se javlja pri Se-S segregaciji**

crystals due to the adsorption the faceting occurred. Grant and Hass observed the faceting of (110) surface of Cr and reconstruction to (100) upon oxygen and carbon monoxide absorption [10]; Russeberg and Viefhaus [11] found faceting of (110) surfaces during Sb segregation.

During the selenium-sulfur co-segregation, the (110) planes of grains at the surface of the sample were observed to facet [9]. These faceted (110) grains showed evidence for surface reconstruction induced by the segregates. Figure 5. shows SEM image of the first state of the surface reconstruction and confirm the suggestion that the process of grain surface reconstruction from (110) to (100) occurred during the Se-S segregation. All of the Auger spectra (not presented in the article) taken in the positions P_1 - P_4 show a homogenous ultra thin segregated film of Se and S. This layer induces the grain reconstruction.

Inclusions
in resulfurized continuous casting steel billets

The quality of resulfurized steels with a sulfur content over 0.025 wt % and 0.02 - 0.04 wt % aluminium is strongly dependent on kind, size and distribution of inclusions [10]. Figure 6. shows a SEM image of an inclusion [13]. The

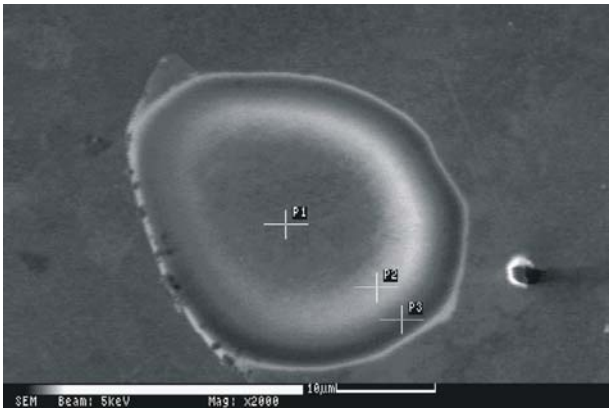

Figure 6. **SEM image of the CaS-CaO inclusion with marked (P_1, P_2 and P_3) position of AES analysis**
Slika 6. **SEM slika CaS-CaO uključka s naznačenim položajem (P_1, P_2 i P_3)AES analize**

inclusion was analyzed at several positions, as indicated in the figure. In Figure 7. the Auger spectra measured in the points P_1, P_2 and P_3 are shown. From these Auger spectra it was estimated that the inclusion is a mixture of CaO and CaS or of a compound containing those elements. In the central area also iron was found. The distribution of Ca, S and O within the inclusion is homogenous up to the limit of geometrical resolution of HRAES. This is shown in Figure 8. where Scanning Auger Mapping (SAM) images for Ca, O, and S, respectively, are presented. Note that these images show the inclusion and the matrix around it. If the inclusion would be a combination of coarse segregated clusters of CaO and CaS or CaO and Fe rather than of compound their distribution across the inclusion surface should be inhomogeneous. In addition, only the central area of the inclusion (P_1) contains a significant amount of iron that is otherwise the main component of the matrix. Most probably, this iron layer influences the chemical composition of the inclusion which is not homogenous when judged from the spectra shown in Figure 7.: while all spectra contain calcium, oxygen and sulfur

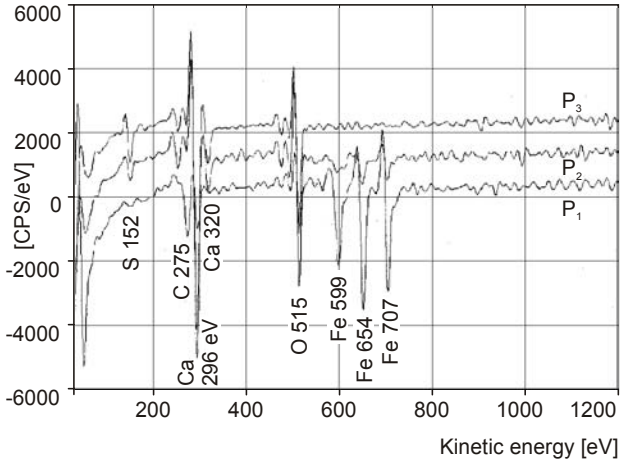

Figure 7. **AES spectra measured in points (P_1-P_2-P_3) showed in SEM image (Figure 6)**
Slika 7. **AES spektri mjereni u točkama (P_1-P_2-P_3) predočenim u SEM slici (Slika 6)**

their mutual ratios differ considerably from one point of the analysis to the other and this is directly connected with the amount of iron signal in the spectra.

Oxide scale formation by
decarburization of non-oriented electrical steel sheets

In Figure 9a., SEM image of oxide layer after decarburization annealing at 840 °C in the gas mixture of H_2-H_2Ov-N_2, is shown[14]. The thickness of the oxide layer was about 1 mm and it is evident that the oxide scale is porous. AES spectra of the same area are shown in Figure 9b. AES and XPS analysis confirmed Fe_3O_4 on the surface and showed no Si and/or Al in the oxide layer. An oxide layer of 3 mm thickness was formed after decarburization annealing first at 840 °C in the equal gas mixture and then in a H_2-N_2 gas mixture at 1050 °C. During the decarburization process carbon oxidized to CO and CO_2 and the oxide layer split into a double-layered scale. Upon the subsequent cooling the major part of the upper oxide layer was scaled off.

In Figure 10a. an SEM image of oxide layer on the strip surface of the steel is shown. It is evident that oxide layer is partly porous and partly compact. AES analysis was performed in the positions P_1, P_2 and P_3. In Figure 10b. AES spectra measured in P_1 and P_2 show that the com-

pact oxide is most probably a mixture of Fe_2SiO_4 (Fayalite) and $FeAl_2O_4$, (Hercynite), while in P_3 only Fe_2SiO_4 is present, which is porous, as is it shown in SEM image.

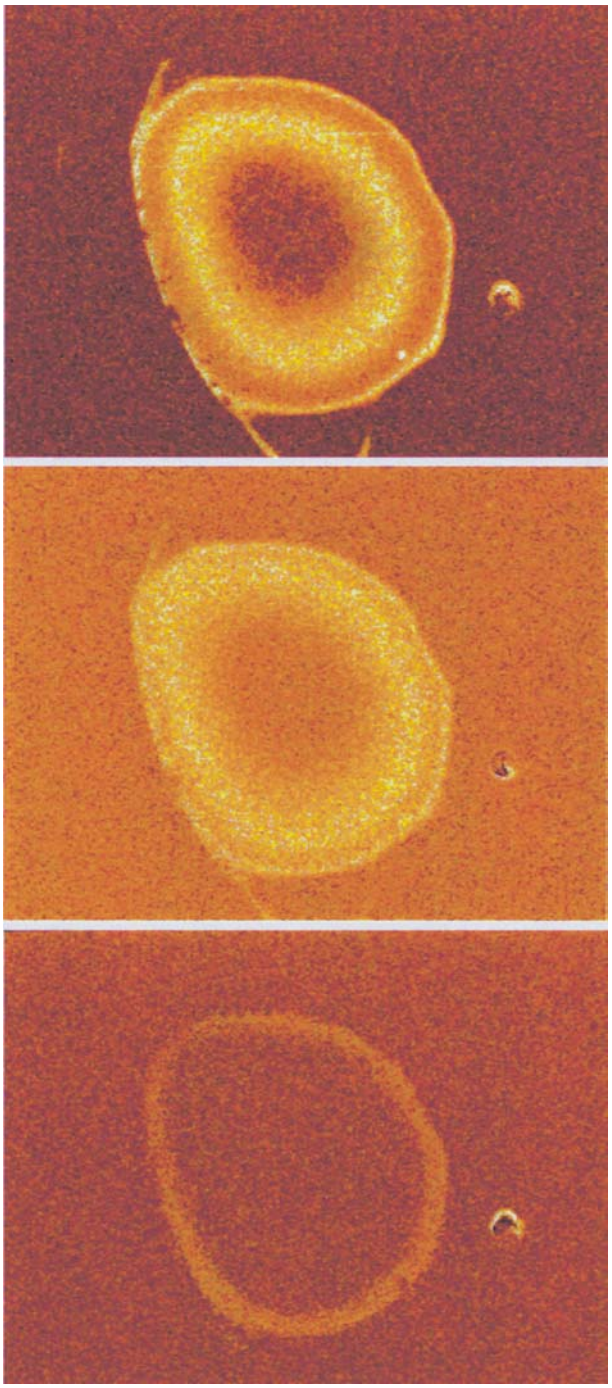

Figure 8. **a) Scanning Auger Mapping (SAM) image of calcium distribution in the inclusion showed in Figure 6.;**
b) SAM image of oxygen distribution in the inclusion;
c) SAM image of sulfur distribution in the inclusion
Slika 8. **a) Auger-ovo mapiranje (SAM) raspodjele kalcija u uključku predočenom na Slici 6.;**
b) SAM-slika raspodjele kisika u uključku;
c) SAM-slika raspodjele sumpora u uključku

The XPS analysis confirmed Fayalite presence on the surface. It is known that the formation of Fayalite during the final heat treatment of non oriented electrical steel sheets retards the decarburization process [15-22].

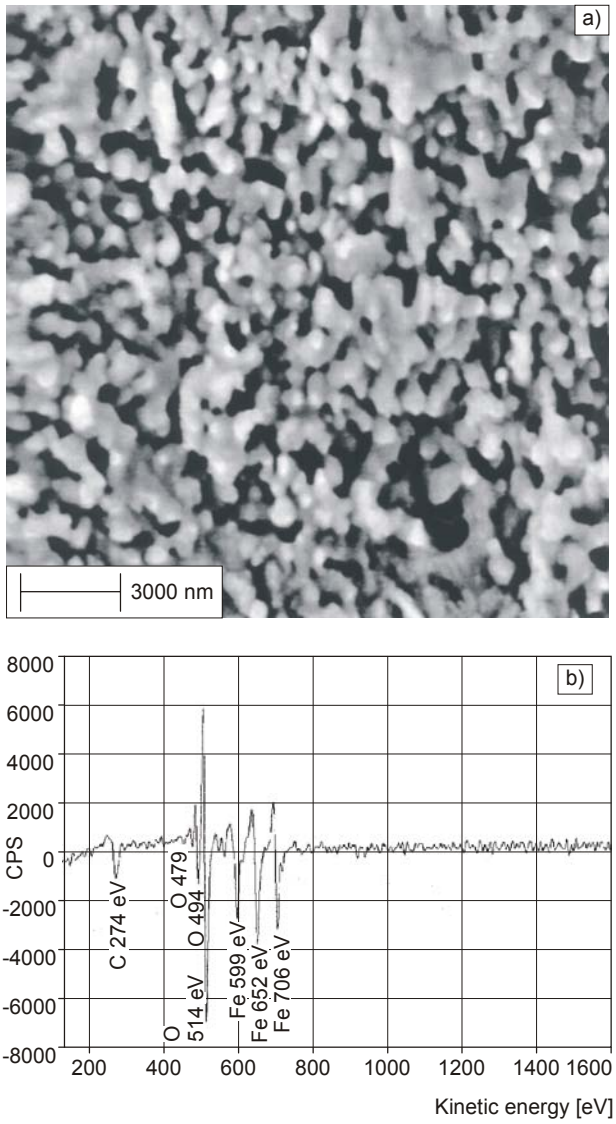

Figure 9. **a) SEM image of oxide layer after decarburization at 840 °C in the gas mixture of H_2-H_2O-N_2, T_{dp} = 40 °C;**
b) AES spectra of the same oxide layer
Slika 9. **a) SEM slika oksidnog sloja nakon dekarburizacije pri 840 °C u plinskoj smjesi H_2-H_2O-N_2, T_{dp} = 40 °C;**
b) AES spektar istog oksidnog sloja

Interfacial study of 19Cr-13Ni austenitic stainless steel after treatment at elevated temperatures

The samples of investigated steel, alloyed by P, were heat treated and inserted into the preparation chamber of the spectrometer where they were fractured in ultra high vacuum environment [23]. On fracture surfaces two types

of facets were observed: intergranular ones with dimple morphology and transgranular cleavage-like ones. On intergranular facets a number of inclusions was found (Figure 11a.). The Auger spectra were taken at representative

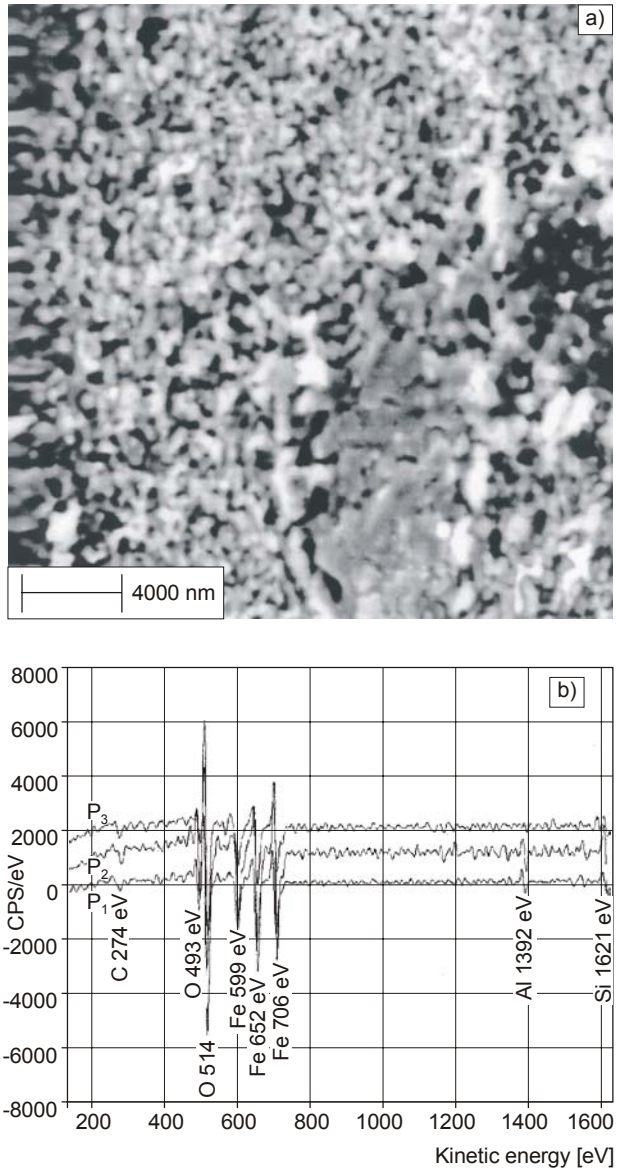

Figure 10. **a) SEM image of the oxide layer on the surface of the steel, the layer is porous and compact only on some areas; b) AES spectra measured in P_1 and P_2 showed that the compact oxide layer is a mixture of Fe_2SiO_4 - Fayalite and $Fe_2Al_2O_4$ - Hercynite**

Slika 10. **a) SEM slika oksidnog sloja na površini čelika, sloj je porozan a u nekim dijelovima kompaktan; b) AES spektri mjereni u P_1 i P_2 u ukazuju da je kompaktni oksidni sloj smjesa Fe_2SiO_4 - fajalita i $Fe_2Al_2O_4$ - hercinita**

points of the sample as indicated in the image. The grains (average size of 256 mm) formed during the heat treatment were found to be large enough for satisfactory analysis of observed facets to be made. The AES spectra contained peaks of Fe, Cr, C, P, S, and O. An occurrence of

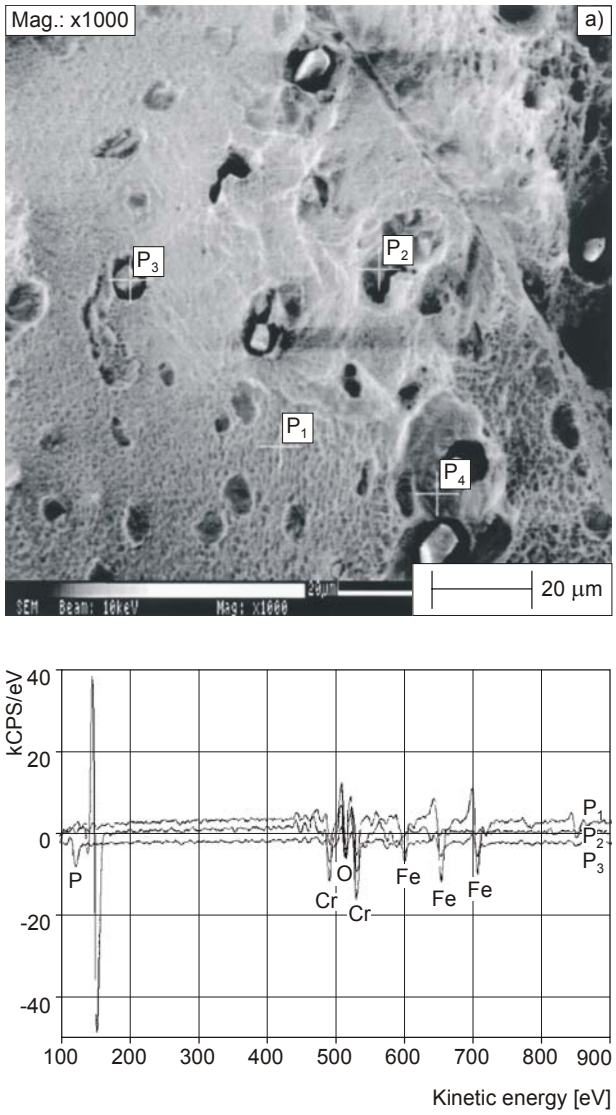

Figure 11. **Intergranular facet on fracture surface of sample annealed at 800 °C for 100 h: a) SEM image; b) Auger spectrum of P_1 with low P and C peaks; c) Auger spectrum of P_2 with high S peak; d) Auger spectrum of P_3 with high P and Cr peaks**

Slika 11. **Intergranularna ploha (facet) prelomne površine uzorka napuštanog 100 h na 800 °C: a) SEM slika; b) Auger-ov spektar u P_1 s malim P i C vrhovima; c) Auger-ov spektar u P_2 s velikim S vrhom; d) Auger-ov spektar u P_3 s velikim P i Cr vrhovima**

the oxygen peak in all Auger spectra was caused by adsorption from residual atmosphere or by presence of oxide inclusions on intergranular facets. The full advantage of the nanospot Auger spectrometry is seen in Figure 12. where structural details well below 1 μm may be easily analyzed to ascertain their chemical composition.

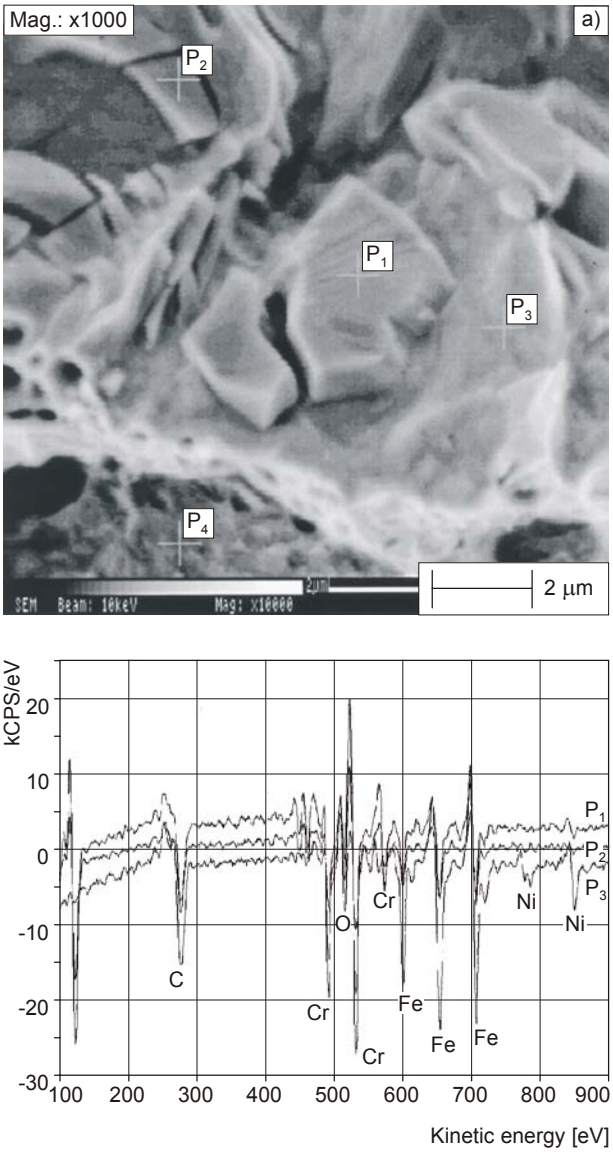

Figure 12. **Intergranular facet on fracture surface of sample aged at 800 °C for 1000 h:**
a) SEM image of intergranular particles;
b) Auger spectrum of particle P_1 showing high P, C, and Cr peaks;
c) Auger spectrum of particle P_2 showing high P, C, and Cr peaks;
d) Auger spectrum of P_3 without P and Cr peaks

Slika 12. **Intergranularna ploha (facet) prelomne površine uzorka starenog 1000 h na 800 °C:**
a) SEM slika međugranularnih čestica;
b) Auger-ov spektar čestice P_1 koja ukazuje na visoke P, C i Cr vrhove
c) Auger-ov spektar čestice P_2 koja ukazuje na visoke P, C i Cr vrhove
d) Auger-ov spektar čestice P_3 bez P, C i Cr vrhova

CONCLUSIONS

It may be concluded that the high spatial resolution Auger electron spectroscopy is a very powerful tool to study a large number of problems frequently encountered in metallurgy. In many cases a combination of HRAES and X-ray photoelectron spectroscopy presents the only choice to resolve the nature of various ingredients of a metallic specimen. This does not apply exclusively to surface problems, for in those cases where the fracture of a specimen in high vacuum conditions was possible the freshly produced surfaces reveal the chemical composition of the interior of the grains and between the grains.

REFERENCES

1. D. Briggs, M. P. Seah: Practical Surface Analysis, 2nd ed., J. Wiley & Sons, Chichester, 1994
2. C. L. Hedberg Ed, Handbook of Auger Electron Spectroscopy 3rd ed., Physical Electronics, Eden Prairie, Minnesota, 1995
3. M. Thompson, M. D. Baker, A. Christie, J. F. Tyson: Auger Electron Spectroscopy, John Wiley & Sons, NY 1985
4. J. Chastain, R. C. King (Eds), Handbook of X-ray Photoelectron Spectroscopy, Physical Electronics, Eden Praire, Minesota, 1995
5. H. J. Grabke: Iron Steel J. 35 (1995) 95
6. H. J. Grabke: Impurities in Engineering Materials, Briant CL(Ed.), Marcel Dekker, New York, 1999, 143.
7. M. Jenko, J. Fine, D. Mandrino: Kov. Zlit. Tehnol. 32 (1998) 437
8. M. Godec, M. Jenko, H. J. Grabke, R. Mast: Iron Steel J. 39 (1999) 742
9. M. Jenko, J. Fine and D. Mandrino: Surf. Interface Anal. 30 (2000) 350
10. J. T. Grant and T. W. Haas: Surf. Sci. 17 (1969) 484
11. V. Rusenberg and H. Viefhaus: Surf. Sci. 172 (1986) 615
12. B. Hoh, H. Jacobi, H. E. Wiemer, K. Wünnenberg: Stahl und Eisen 109 (1989) 69
13. B. Koroušič and M. Jenko: Steel Res. 73 (2002) 63
14. M. Jenko, B. Koroušič, D. Mandrino and V. Prešern: Vacuum 57 (2000) 295
15. Koroušić B., Kov. Zlit. Tehnol. 28 (1994) 609
16. Koroušić B., Rosina A., RadexRundsch. 1 (1994) 523
17. L. L. Shreier, R. A. Jarman, G. T. Burstein: Corrosion: Vol. 1 Metal/ Environment Reactions, Third Edition, Butterworth-Heinemann: Oxford 1995
18. H. J. Grabke, G. Tauber: Arch. Eisenhüttenwes 46 (1975) 215
19. W. F.Block, N. Jayaroman: Materials Science Technology 2 (1986) 22
20. R. W. Gurry, A. Trans: 188 (1950) 671
21. T. Nada, M. Okada, R. Wafarable: Metal Trans. B 11 (1980) 331
22. D. Steiner Petrovič, M. Jenko, V. Gontarev, H. J. Grabke, Kov. Zlit. Tehnol. 32 (1998) 493
23. P. Ševc, D. Mandrino, J. Blach, M. Jenko, J. Janovec: Kovove Materiali 40 (2002) 35